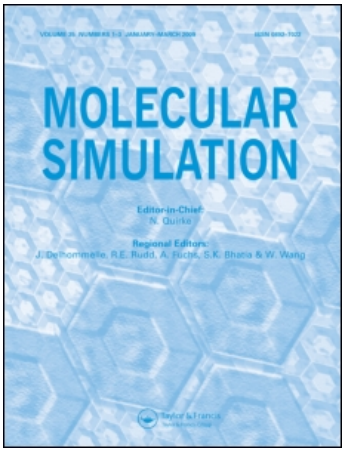

Molecular Simulation
Publication details, including instructions for authors and subscription information:
http://www.informaworld.com/smpp/title~content=t713644482

Compact model of the quantum short-channel threshold voltage in symmetric Double-Gate MOSFET

D. Munteanu[a]; J. L. Autran[b]; S. Harrison[c]; K. Nehari[a]; O. Tintori[a]; T. Skotnicki[c]
[a] L2MP, Bâtiment IRPHE, Marseille cedex 13, France [b] Institut Universitaire deFrance—IUF, France [c] STMicroelectronics, Crolles, France

To cite this Article Munteanu, D. , Autran, J. L. , Harrison, S. , Nehari, K. , Tintori, O. and Skotnicki, T.(2005) 'Compact model of the quantum short-channel threshold voltage in symmetric Double-Gate MOSFET', Molecular Simulation, 31: 12, 831 — 837
To link to this Article: DOI: 10.1080/08927020500313995
URL: http://dx.doi.org/10.1080/08927020500313995

Molecular Simulation, Vol. 31, No. 12, 15 October 2005, 831–837

Taylor & Francis
Taylor & Francis Group

Compact model of the quantum short-channel threshold voltage in symmetric Double-Gate MOSFET

D. MUNTEANU†*, J. L. AUTRAN†‡, S. HARRISON†¶, K. NEHARI†, O. TINTORI† and T. SKOTNICKI¶

†L2MP, Bâtiment IRPHE, 49 rue Joliot-Curie, BP 146, F-13384, Marseille cedex 13, France
‡Institut Universitaire deFrance—IUF, France
¶STMicroelectronics, 850 rue J. Monnet, 38926 Crolles, France

(Received June 2005; in final form August 2005)

A compact model for the threshold voltage in Double-Gate (DG) MOSFET is developed. The model takes into account short-channel effects, carrier quantization and temperature dependence of the threshold voltage. We assume a parabolic variation of the potential with the vertical position in the silicon film at threshold. An analytical expression for the surface potential dependence as a function of bias and position in the silicon film is also developed and used for the inversion charge calculation. The model has been fully validated by 2D quantum numerical simulation and is used to predict the threshold voltage roll-off in DG MOSFET with very short channel lengths and thin films. The comparison with measured threshold voltages shows that the model reproduces with an excellent accuracy the experimental data.

Keywords: Compact modeling; Threshold voltage; Double-Gate MOSFET; Short-channel effects; Quantum effects

1. Introduction

Compact modeling of Double-Gate (DG) MOSFET incites very much interest presently, since DG structure is considered to be one of the best device architectures, not only for MOSFET integration in the Silicon technology end-of-roadmap perspective but also for future possible post-CMOS molecular-based devices [1,2]. The main advantage of this architecture is to offer a reinforced electrostatic coupling between the conduction channel and the gate electrode. In other terms, a DG structure can efficiently sandwich (and thus very well control, electrostatically speaking) the semiconductor element playing the role of the transistor channel, which can be a Silicon thin layer or nano-wire, a Carbon nano-tube, a molecule or an atomic linear chain. The MOSFET operation of such ultimate DG devices with a single quantum conduction channel has been theoretically demonstrated in recent works [3,4].

For conventional Silicon CMOS-based devices, modeling of the threshold voltage (V_T) in the DG MOSFET is a difficult task because the usual definition of the threshold voltage (i.e. for bulk devices) does not more apply [5,6]. Several analytical models have been derived previously for the threshold voltage [4,6–9], but most of them apply only in particular cases or neglect essential physical phenomena as discussed in the following:

(1) Existing V_T models have been developed only for devices with undoped channels because DG devices are expected to be designed with intrinsic channels in order to enhance the carrier mobility and solve the problem of doping induced parameter fluctuation. However, the use of undoped channel in symmetric DG will need the use of midgap gates (because devices with $n+$ poly gates have negative threshold voltage) which is an important technological challenge. Presently, most of DG MOSFETs are fabricated with doped channel and $n+$ poly gates and, therefore, a V_T model applying for both doped and undoped channel is needed.
(2) Most of the existing V_T models are based on a one-dimensional analysis which is only suitable for long channel devices. Since DG structure will be mainly used to design very scaled devices, 2D electrostatics is key-phenomenon which has to be taken into account.
(3) Quantum effects are often neglected (or only roughly estimated) in the development of V_T models and, therefore, these models could be applied only for silicon channels thicker than 10 nm.

*Corresponding author. Tel.: +33-4-96-13-98-19. Fax: +33-4-96-13-97-09. Email: munteanu@newsup.univ-mrs.fr

Molecular Simulation
ISSN 0892-7022 print/ISSN 1029-0435 online © 2005 Taylor & Francis
http://www.tandf.co.uk/journals
DOI: 10.1080/08927020500313995

The aim of this work is to develop a short-channel quantum mechanical compact model for threshold voltage based on the decoupled Poisson and Schrödinger equations in the silicon film. Recently, we have proposed an analytical V_T model for long channel devices including quantum effects and applying to both symmetric and asymmetric device [10]. This model is enhanced in this work for taking into account short channel effects and temperature dependence of V_T. The model is completely validated using a full 2D quantum mechanical numerical simulation code [11] and is compared with experimental data extracted from DG devices fabricated using the SON/DG process [12]. We present here the model development in the case of a symmetric DG device, but it can be very easily adapted to any asymmetric DG device (different oxides thicknesses or gate work-functions).

2. Threshold voltage definition

Figure 1a shows the schematic of a symmetric DG structure and the variation of the surface potential Ψ_s in a horizontal cross-section in the channel (figure 1b). A parabolic dependence for the potential, at threshold, in the vertical direction is assumed [5] (figure 1c):

$$\Psi(x, y) = \Psi_s(x) - \alpha(x) t_{Si} y + \alpha(x) y^2 \tag{1}$$

where the calculation of $\alpha(x)$ is indicated in paragraph 4. It is important to note that equation (1) is valid at threshold, but could lose its validity in other operation regimes (such as the strong inversion regime). The boundary conditions at the Si/SiO_2 interface are:

$$V_G - V_{FB} = \frac{\varepsilon_{Si}}{\varepsilon_{ox}} t_{ox} \xi_s + \Psi_s + \phi_F \tag{2}$$

where Ψ_S and ξ_S are the potential and, respectively, the electric field at the interface and $\phi_F = (kT/q)\ln(N_A/n_i)$ is the Fermi potential (N_A is the doping level in the Si film). Potential Ψ and the semiconductor charge (including both the depletion and mobile charges) in the Si film are linked via the Poisson equation:

$$\frac{d^2\Psi}{dy^2} = \frac{qN_A}{\varepsilon_{Si}} + \frac{q}{\varepsilon_{Si}} n_i \exp\left(\frac{q\Psi}{kT}\right) \tag{3}$$

In the right side of equation (3), the first term represents the depletion charge and the second term is the mobile charge in the silicon film. We consider here that the silicon film is always depleted. For defining V_T, it is important to remind that in DG MOSFET the usual definition of the V_T as the gate voltage where Ψ_s is $2\phi_F$ does no more apply [5,6]. Our extensive numerical simulation fully confirms this remark and shows that surface potential at threshold, Ψ_s, is different from ϕ_F (table 1). Other definitions for the threshold voltage exist, as derived from the constant-current method or the maximum of d^2I_D/dV_G^2. In a recent work [13], we used this latter criterion, but the resulting analytical expression of the threshold voltage is quite complicated and its demonstration demands heavy mathematical manipulations. For obtaining a more simple expression of V_T, we define here V_T as the gate voltage for which the inversion

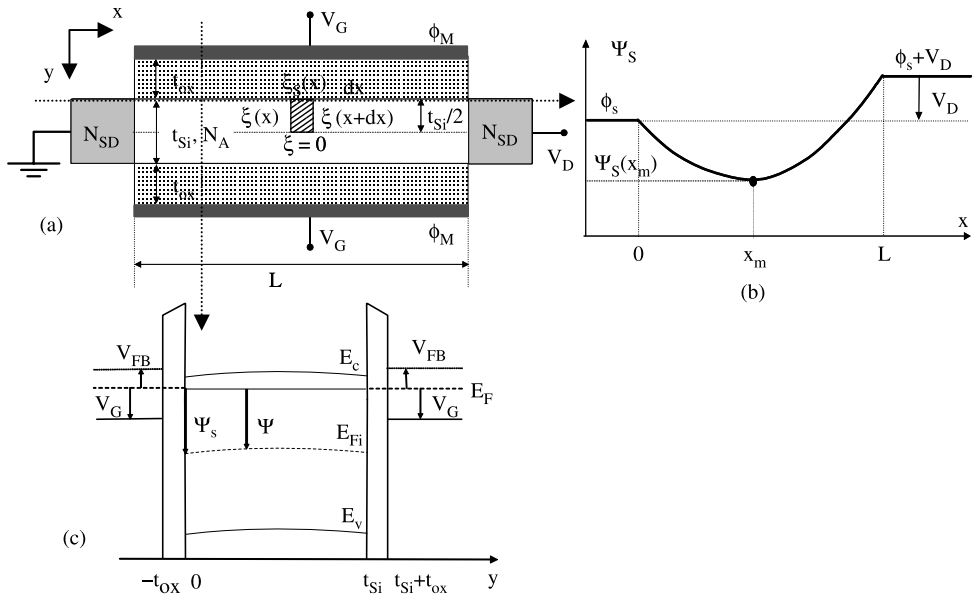

Figure 1. (a) Schematic symmetric DG MOSFET structure and its electrical and geometrical parameters considered in this work; the dashed area shows the closed surface for the application of the Gauss's law; (b) Surface potential variation in the x direction from the source-to-drain; (c) Band diagram in a vertical cross-section in the channel and definition of the different parameters used in the model development.

Table 1. Surface potential extracted from numerical simulation for symmetric DG with midgap gates, with different film thicknesses and doping levels. The surface potential is different from ϕ_F in all cases.

	N_A (cm^{-3})	t_{Si} (nm)	Ψ_s (V) (numerical simulation)	ϕ_F (V)
Symmetric DG midgap gates	1×10^{16}	5	0.487	
		10	0.468	0.368
		15	0.458	
	1×10^{18}	5	0.49	
		10	0.484	0.487
		15	0.483	

charge, Q_i, reaches a constant value:

$$Q_T = \frac{kT}{q} C_{ox} \tag{4}$$

3. Long channel threshold voltage

In a long channel device, it can be assumed that the surface potential is constant along the channel (far from the source and drain contacts). Therefore, equation (1) becomes:

$$\Psi(y) = \Psi_s - \alpha t_{Si} y + \alpha y^2 \tag{5}$$

where the parameter α will be calculated in the following. From equation (5) the electric field at the Si/SiO_2 interfaces is:

$$\xi = -\frac{d\Psi}{dy}\Big| y = 0, t_{Si} = \alpha t_{Si} \tag{6}$$

Integrating equation (3) from $y = 0$ to $y = t_{Si}$ gives:

$$\xi = \frac{qN_A t_{Si}}{2\varepsilon_{Si}} + \frac{Q_i}{2\varepsilon_{Si}} \tag{7}$$

where Q_i is the density of inversion charge in the silicon film:

$$Q_i = \int_0^{t_{Si}} q\, n_i\, e^{\frac{q\Psi(y)}{kT}} dy \tag{8}$$

From equations (6) to (8), the expression of parameter α is obtained as a function of Q_i:

$$\alpha = \frac{qN_A}{2\varepsilon_{Si}} + \frac{Q_i}{2\varepsilon_{Si} t_{Si}} \tag{9}$$

The surface potential Ψ_s can be expressed as a function of Q_i from equations (8) and (3) as:

$$\Psi_s = u_{th} \ln\left(\frac{Q_i}{q\, n_i \int_0^{t_{Si}} e^{\frac{1}{u_{th}}(-\alpha t_{Si} y + \alpha y^2)} dy}\right) \tag{10}$$

where α is function of Q_i (relation (9)) and $u_{th} = kT/q$. The expression

$$\int_0^{t_{Si}} e^{\frac{1}{u_{th}}(-\alpha t_{Si} y + \alpha y^2)} dy$$

can be expressed analytically using the imaginary error function $Erfi(x) = (2/\sqrt{\pi})\int_0^x e^{t^2} dt$ [14]:

$$\int_0^{t_{Si}} e^{\frac{1}{u_{th}}(-\alpha t_{Si} y + \alpha y^2)} dy = e^{-\frac{t_{Si}\alpha}{4u_{th}}} \sqrt{\frac{\pi u_{th}}{\alpha}} Erfi\left(\frac{t_{Si}}{2}\sqrt{\frac{\alpha}{u_{th}}}\right) \tag{11}$$

Therefore, surface potential can be rewritten as:

$$\Psi_s = u_{th} \ln\left(\frac{Q_i}{qn_i}\right) + \frac{\alpha t_{Si}^2}{4} - \Psi_1 \tag{12}$$

where

$$\Psi_1 = u_{th} \ln\left[\sqrt{\frac{\pi u_{th}}{\alpha}} Erfi\left(\frac{t_{Si}}{2}\sqrt{\frac{\alpha}{u_{th}}}\right)\right] \tag{13}$$

With the condition $Q_i = Q_T$, α and Ψ_s can be now expressed as:

$$\alpha = \frac{qN_A}{2\varepsilon_{Si}} + \frac{kT}{2q}\frac{1}{\gamma t_{ox} t_{Si}} \tag{14}$$

$$\Psi_s = \phi_F + \frac{kT}{q} \ln\left[\frac{kTC_{ox}}{q^2 N_A}\right] + \frac{\alpha t_{Si^2}}{4} - \Psi_1 \tag{15}$$

where $\gamma = \varepsilon_{Si}/\varepsilon_{ox}$. Combining equations (1)–(3) and equation (15) the expression of the threshold voltage in a long channel device is obtained:

$$V_T = V_{FB} + \frac{qN_A t_{Si}}{2C_{ox}} + \frac{kT}{q} \ln\left[\frac{kTC_{ox}}{q^2 N_A}\right] + \frac{\alpha t_{Si^2}}{4} - \Psi_1 + 2\phi_F \tag{16}$$

This equation is completely analytical and applies for all symmetric DG devices, with both doped and undoped channels.

4. Quantum effects

The introduction of quantum effects requires a new calculation of the inversion charge Q_i using the following quantum-mechanically evaluation:

$$Q_i = \frac{qkT}{\pi\hbar^2}\sum_{l,t}\sum_i m_{2D}^{t,l} g_{t,l} \times \ln\left[1+\exp\left(-\frac{1}{u_{\text{th}}}\left(\tilde{E}_{l,t}^i + \frac{E_g}{2} - \Psi_s\right)\right)\right] \quad (17)$$

where the following parameter values apply for Silicon: $m_{2D}^1 = m_t^*$, $m_{2D}^t = \sqrt{m_1^* m_t^*}$, $m_t^* = 0.19 \times m_0$, $m_1^* = 0.98 \times m_0$, $g_l = 2$, $g_t = 4$. In equation (17) Ψ_s is the surface potential and $\tilde{E}_{l,t}^i$ are the energy levels resulting from the quantum confinement of carriers in the film perpendicular to the channel. For calculating $\tilde{E}_{l,t}^i$ we consider in a first approximation that the band diagram in symmetric DG structure is close to an infinite rectangular well. The energy levels are then given by:

$$E_{l,t}^i = \frac{\hbar^2\pi^2 i^2}{2qm_{l,t}^* t_{\text{Si}}^2} \quad (18)$$

In a second step, a more carefully evaluation of these energy levels can be performed using a standard method for first-order perturbation [10]. Considering the parabolic nature of the potential profile in the Si film, as described by equation (5), the first-order correction to apply to the energy levels in the well is given by:

$$\Delta E^i = \langle \varphi^i | H | \varphi^i \rangle \quad (19)$$

where $H = -q(-\alpha t_{\text{Si}} y + \alpha y^2)$ is the Hamiltonian of the perturbation and ϕ^i are the electron wave functions associated to energy levels $E_{l,t}^i$. Finally, the first-order corrected energy levels are given by:

$$\tilde{E}_{l.t}^i = E_{l,t}^i + \Delta E^i \quad (20)$$

Due to the analytical character of both ϕ^i and H, the analytical calculation of equation (19) gives ΔE^i in the case of an infinite rectangular well subjected to the considered perturbation:

$$\Delta E^i = \frac{\alpha t_{\text{Si}}^2}{6}\left[1+\frac{3}{\pi^2 i^2}\right] \quad (21)$$

Finally, the corrected energy levels are given by the following equation:

$$\tilde{E}_{l,t}^i = \frac{\hbar^2\pi^2 i^2}{2qm_{l,t}^* t_{\text{Si}}^2} + \frac{\alpha t_{\text{Si}}^2}{6}\left[1+\frac{3}{\pi^2 i^2}\right] \quad (22)$$

5. Short-channel effects

In a short channel device, the surface potential is no longer constant and depends on the position in the channel, x. Therefore, parameter α becomes dependent on x, as well as the energy levels and the inversion charge. In the following, we develop the expression of $\Psi_s(x)$ which will be used further for calculating $\alpha(x)$, $\tilde{E}_{1,t}^i(x)$ and $Q_i(x)$. For this purpose, the Gauss's law is applied to the particular closed surface shown in figure 1a:

$$-\xi(x)\frac{t_{\text{Si}}}{2} + \xi(x+\mathrm{d}x)\frac{t_{\text{Si}}}{2} - \xi_s(x)\mathrm{d}x = -\frac{qN_A t_{\text{Si}}}{2\varepsilon_{\text{Si}}} \quad (23)$$

The electric field $\xi(x)$ can be approximated by:

$$\xi(x) \approx -\frac{1}{\eta}\frac{\mathrm{d}\Psi_s(x)}{\mathrm{d}x} \quad (24)$$

where η is a fitting parameter which incorporates the effects of the variation of the lateral field in the depleted film under the channel [15,16]. As demonstrated in [15], η is lower than 1 for $V_G = V_T$ and depends on the channel doping and thickness. Therefore, this parameter has to be calibrated for each particular technology. After some algebraic manipulations and using equation (2) the following differential equation is obtained for the surface potential:

$$\frac{\mathrm{d}^2\Psi_s}{\mathrm{d}x^2} - \frac{2\eta C_{\text{ox}}}{\varepsilon_{\text{Si}} t_{\text{Si}}}\Psi_s = \frac{\eta}{\varepsilon_{\text{Si}} t_{\text{Si}}} \times \left[qN_A t_{\text{Si}} - 2C_{\text{ox}}(V_{GS} - V_{FB} - \phi_F)\right] \quad (25)$$

The analytical solution of equation (25) is given by:

$$\Psi_s(x) = C_1\exp(m_1 x) + C_2\exp(-m_1 x) - \frac{R}{m_1^2} \quad (26)$$

with coefficients C_1, C_2, m_1 and R given by:

$$C_1 = \frac{\phi_S[1-\exp(-m_1 L)] + V_D + R\frac{1-\exp(-m_1 L)}{m_1^2}}{2\sin h(m_1 L)} \quad (27)$$

$$C_2 = -\frac{\phi_S[1-\exp(m_1 L)] + V_D + R\frac{1-\exp(m_1 L)}{m_1^2}}{2\sin h(m_1 L)} \quad (28)$$

$$R = \eta\frac{qN_A t_{\text{Si}} - 2C_{\text{ox}}(V_G - V_{FB} - \phi_F)}{\varepsilon_{\text{Si}} t_{\text{Si}}} \quad (29)$$

$$m_1 = \sqrt{\frac{2\eta C_{\text{ox}}}{\varepsilon_{\text{Si}} t_{\text{Si}}}} \quad (30)$$

$$\phi_S = \frac{kT}{q}\ln\left(\frac{N_A N_{SD}}{n_i^2}\right) \quad (31)$$

The variation of the surface potential as described by relation (26) is schematically shown in figure 1b. Combining equations (2) and (6), the expression of the parameter $\alpha(x)$ is easily obtained:

$$\alpha(x) = \frac{1}{\gamma t_{\text{Si}} t_{\text{ox}}}(V_G - V_{FB} - \phi_F - \Psi_s(x)) \quad (32)$$

The energy levels $\tilde{E}_{1,t}^i(x)$ are then calculated using relations (22) and (32). The quantum short-channel

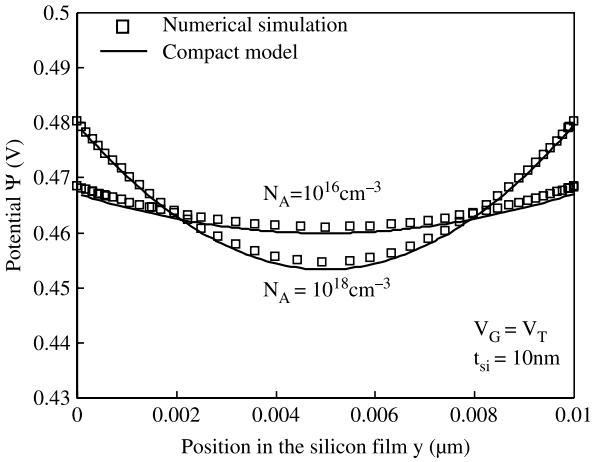

Figure 2. Variation of the potential in a vertical cross-section in the channel as predicted by the compact model and comparison with numerical simulation.

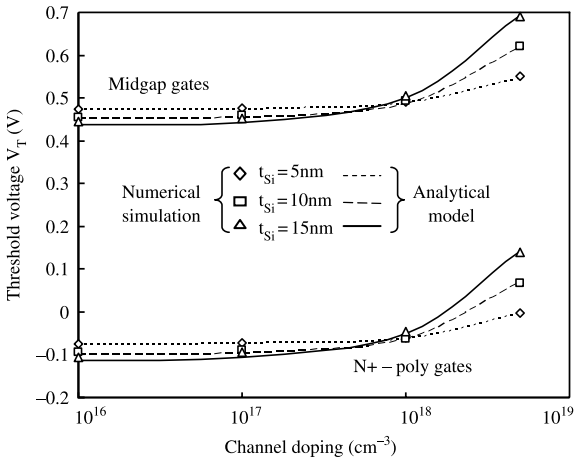

Figure 4. Comparison between threshold voltages obtained with analytical model and numerical simulation in long channel DG devices (with midgap and $n+$ poly gates, $t_{ox} = 1$ nm, $V_D = 0.1$ V).

inversion charge $Q_i(x)$ will be given by:

$$Q_i(x) = \frac{qkT}{\pi\hbar^2}\sum_{l,t}\sum_{i} m_{2D}^{t,l} g_{t,l} \times \ln\left[1+\exp\left(-\frac{1}{u_{th}}\left(\tilde{E}_{l,t}^{i}(x)+\frac{E_g}{2}-\Psi_s(x)\right)\right)\right] \quad (33)$$

Finally, for calculating the threshold voltage we consider that the transistor is composed from a finite number of elementary transistors corresponding to each x point. The threshold voltage V_T of the whole transistor is given by the V_T of the transistor which lastly turns-on. This particular transistor is evidently the one located at the point $x = x_m$ where the surface potential is minimum. The point x_m is the solution of the equation $d\Psi_s/dx = 0$, which gives:

$$x_m = \frac{1}{2m_1}\ln\left(\frac{C_2}{C_1}\right) \quad (34)$$

The threshold voltage is then calculated by numerically solving the equation:

$$Q_i(x_m) = Q_T \quad (35)$$

.

6. Model validation

The model was validated by an extensive comparison with quantum numerical simulation using a 2D Poisson-Schrödinger code [11] (we used here a quantum drift-diffusion transport model). In a first step, the 2D potential distribution in the film at threshold has been verified.

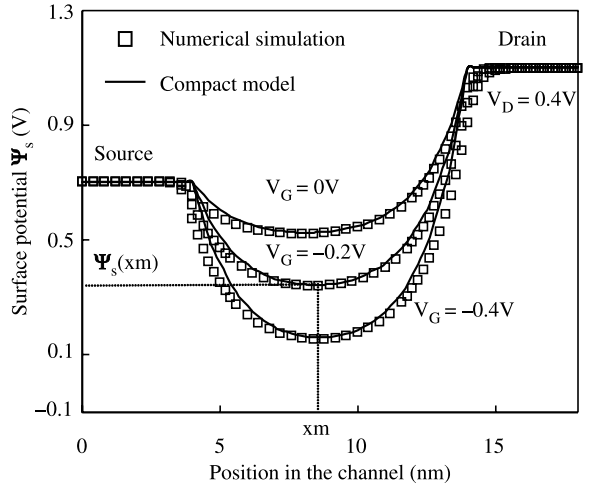

Figure 3. Surface potential Ψ_s variation calculated with the analytical model (relation 26) and comparison with the 2D numerical code.

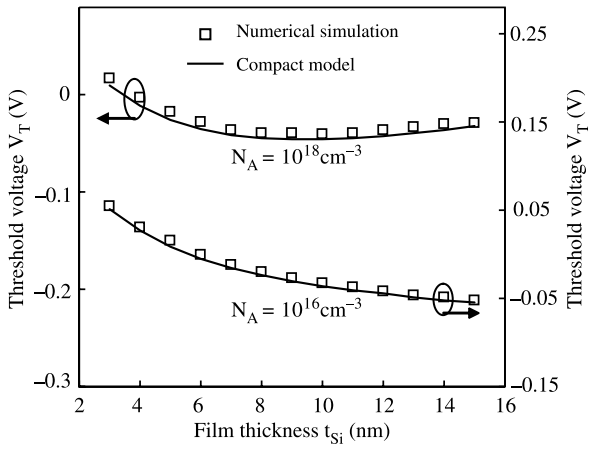

Figure 5. Comparison between V_T given by the quantum compact model and quantum numerical simulation in long channel DG devices with low and high channel doping ($V_D = 0.1$ V).

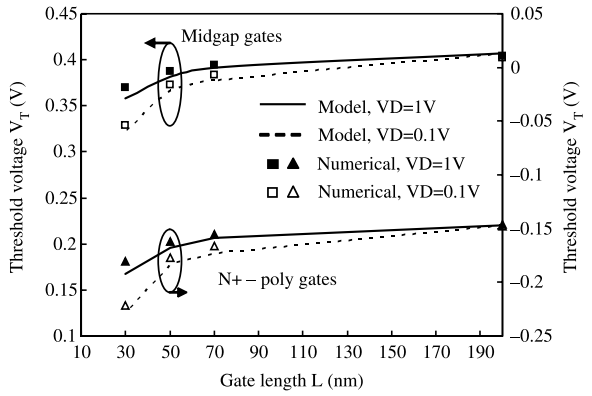

Figure 6. Short-channel V_T given by the compact model and 2D numerical simulation as a function of the channel length and at low and high drain voltage (intrinsic channel, $t_{ox} = 1$ nm, $t_{Si} = 10$ nm, midgap and $n+$ poly gates).

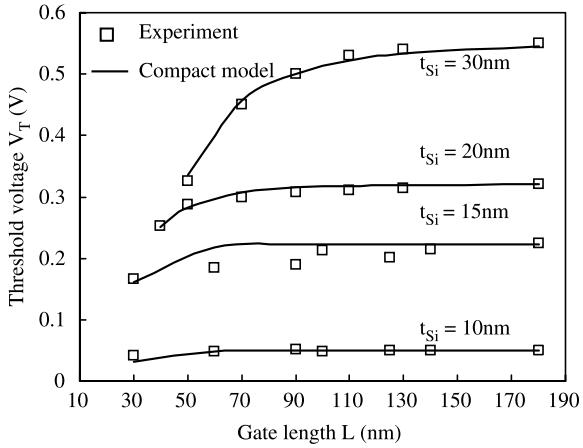

Figure 7. Comparison between measured V_T (on devices described in [12] and table 2) and 2D quantum V_T calculated using the compact model.

Figure 2 shows that the assumption of a vertical parabolic dependence is validated by numerical simulation. The surface potential variation along the x position, given by relation (26), was also confronted to numerical results (for different V_G) in figure 3: the model fits very well the numerical data. In a second step, the threshold voltage model has been completely validated by numerical simulation. Figure 4 shows the comparison between simulation and the model (without quantum effects) in the case of long channel DG devices with both midgap or $n+$ poly gates. An excellent agreement is found for all channel doping levels and film thicknesses. The quantum long channel model is validated by quantum numerical simulation in figure 5 where a very good match is obtained. Figure 6 shows the validation of the model including the short channel effects (induced by both the reduction of the channel lengths and by the increase of the drain voltage); the comparison with threshold voltage extracted from simulated curves at low and high drain voltage indicates that the model reproduces well short-channel and DIBL (Drain Induced Barrier Lowering) effects on the threshold voltage.

7. Comparison with experimental data

Finally, the model was used to fit threshold voltage extracted on DG devices fabricated by SON process, as described in [12]. Devices with different film thicknesses (table 2) have been measured and the threshold voltage has been extracted from the $I_D(V_G)$ characteristics. As shown in figure 7, the match between experiment and model is very satisfactory, showing that the model reproduces well the threshold voltage roll-off of the measured devices. Parameter η, which has been calibrated for each film thickness (table 2), is less than 1 but increases when the film thickness decreases (because the variation of the lateral field in the film becomes less accentuated) and is even equal to 1 for the thinnest film (10 nm).

Moreover, the compact model has been successfully extended in low temperature simply using an appropriate model for the temperature dependence of intrinsic concentration n_i, the effective density-of-states in both conduction and valence bands and the energy bandgap [17]. Figure 8 shows the remarkable fit between the quantum model predicted V_T and the measured V_T in a long channel DG device down to 50 K. This figure illustrates also the necessity to take into account quantum effects in V_T modeling for these very thin devices ($t_{Si} = 10$ nm), since the classical model underestimates the measured data by about 40 mV.

Table 2. Geometrical parameters of the measured DG MOSFET.

Device	t_{Si} *(nm)*	t_{ox} *(Å)*	N_A *(cm^{-3})*	η
A	30	20	$\sim 4 \times 10^{18}$	0.17
B	20	20	$\sim 4 \times 10^{18}$	0.5
C	15	15	$\sim 3.7 \times 10^{18}$	0.6
D	10	15	$\sim 2.5 \times 10^{18}$	1

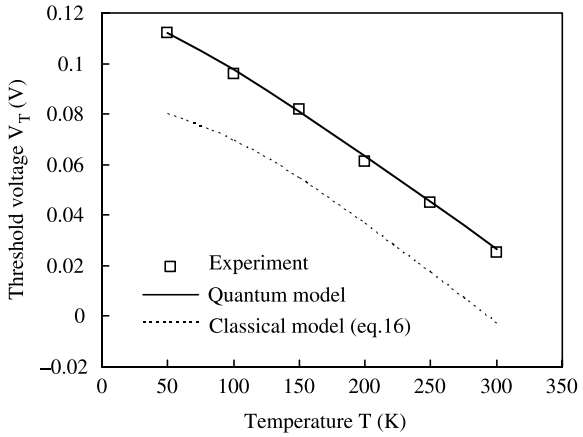

Figure 8. Fit of compact model on measured V_T on a long channel DG device at low temperature ($t_{Si} = 10$ nm, $V_D = 0.1$ V).

8. Conclusion

A new compact model for the threshold voltage in symmetric DG devices has been developed. The model takes into account short-channel effects and quantum confinement of carriers in the direction perpendicular to the channel. The expression of the surface potential as a function of gate and drain biases and of the position in the channel has been developed and integrated in the calculation of the quantum inversion charge. A very satisfactory concordance has been found between the threshold voltage calculated by the compact model and numerical data obtained with a 2D quantum numerical simulation code. Finally, we show that the model provides a very good prediction of the threshold voltage in real devices with different channel thicknesses and gate lengths.

Acknowledgements

This work was supported by the European Commission in the framework of the Network of Excellence on Silicon-based nano-devices (SINANO, contract IST-506844).

References

[1] D.J. Frank, *et al.* Monte Carlo simulation of a 30 nm dual-gate MOSFET: How short can Si go? *IEDM Tech. Dig.*, 553 (1992).
[2] Y. Taur. Analytic solutions of charge and capacitance in symmetric and asymmetric double-gate MOSFETs. *IEEE Trans. Electron. Devices*, **48**, 2861 (2001).
[3] M. Bescond, *et al.* Atomic-scale modeling of source-to-drain tunneling in ultimate Schottky barrier double-gate MOSFET's. *Proc. ESSDERC*, 395 (2003).
[4] M. Bescond, *et al.* Atomic-scale modeling of double-gate MOSFETs using a tight-binding Green's function formalism. *Solid-State Electron.*, **48**, 567 (2004).
[5] K. Nehari, *et al.* Compact modeling of threshold voltage in double-gate MOSFET including quantum mechanical and short channel effects. *Proc. MSM/WCM*, 179 (2005).
[6] Q. Chen, *et al.* Physical short-channel threshold voltage model for undoped symmetric double-gate MOSFETs. *IEEE Trans. Electron. Devices*, **50**, 1631 (2003).
[7] P. Francis, *et al.* Modeling of ultrathin double-gate nMOS/SOI transistors. *IEEE Trans. Electron. Devices*, **41**, 715 (1994).
[8] K. Suzuki, *et al.* Analytical models for n+-p+ double-gate SOI MOSFETs. *IEEE Trans. Electron. Devices*, **42**, 1940 (1995).
[9] X. Liang, Y. Taur. A 2D analytical solution for SCEs in DG MOSFETs. *IEEE Trans. Electron. Devices*, **51**, 1385 (2004).
[10] J.L. Autran, *et al.* Quantum-mechanical analytical modeling of threshold voltage in long-channel double-gate MOSFET with symmetric and asymmetric gates. *Proc. Nanotech/WCM*, 163 (2004).
[11] D. Munteanu, J.L. Autran. Two-dimensional modeling of quantum ballistic transport in ultimate double-gate SOI devices. *Solid-State Electron.*, **47**, 1219 (2003).
[12] S. Harrison, *et al.* Electrical characterization and modelling of high-performance SON DG MOSFETs. *Proc. ESSDERC*, 373 (2004).
[13] D. Munteanu, *et al.* Unified analytical model of threshold voltage in symmetric and asymmetric double-gate MOSFETs. *Proc. ULIS*, 35 (2003).
[14] Mathematica User Manual (2002).
[15] S. Banna, *et al*. Threshold voltage model for deep-submicrometer fully depleted SO1 MOSFET's. *IEEE Trans. Electron. Devices*, **42**, 1949 (1995).
[16] S. Biesemans, *et al*. New current-defined threshold voltage model from 2D potential distribution calculations in MOSFETs. *Solid-State Electron.*, **39**, 43 (1996).
[17] R. Vankemmel, *et al*. Unified wide temperature range model for energy gap, effective carrier mass and intrinsic concentration in silicon. *Solid-State Electron.*, **36**, 1379 (1993).